

High conductive and transparent Al doped ZnO films for a-SiGe:H thin film solar cells

Qingsong LEI (✉), Jiang LI

School of Optical and Electronic Information, Huazhong University of Science and Technology, Wuhan 430074, China

© Higher Education Press and Springer-Verlag Berlin Heidelberg 2014

Abstract Al doped zinc oxide (AZO) films were prepared by mid-frequency magnetron sputtering for silicon (Si) thin film solar cells. Then, the influence of deposition parameters on the electrical and optical properties of the films was studied. Results showed that high conductive and high transparent AZO thin films were achieved with a minimum resistivity of $2.45 \times 10^{-4} \Omega \cdot \text{cm}$ and optical transmission greater than 85% in visible spectrum region as the films were deposited at a substrate temperature of 225°C and a low sputtering power of 160 W. The optimized films were applied as back reflectors in a-SiGe:H solar cells. A relative increase of 19% in the solar cell efficiency was achieved in comparison to the cell without the ZnO films doped with Al (ZnO:Al).

Keywords Al doped zinc oxide (AZO) films, magnetron sputtering technology, growth, electrical and optical properties, a-SiGe:H solar cells

1 Introduction

Transparent conductive oxide (TCO) thin films are widely used in thin film solar cells and flat panel display devices [1–3]. As intermediate or back reflectors in silicon (Si) based thin film solar cells, TCO films with low resistance and high transparency are required to obtain low series resistance and to avoid absorption losses. Compared with other TCO films such as tin-doped In_2O_3 (ITO) and tin oxide (SnO_2), ZnO films doped with Al (ZnO:Al) are more stable in hydrogen plasma environments. Furthermore, ZnO:Al films exhibit high optical transmission and electrical conduction and have a low material cost [4]. These advantages are beneficial for the applications in solar cells and other opto-electronic devices [5–7].

To obtain ZnO:Al films, technologies such as sputtering [8,9], pulsed laser deposition [10], chemical vapor deposition [11], spray pyrolysis [12], and metal-organic chemical vapor deposition (MOCVD) [13] are usually applied. For the above technologies, there are two ways to apply TCO coatings to glass. One is online process and the other is off-line process. During the pyrolytic (online) process, the coating is applied during float glass production. The off-line process occurs after the glass has been produced. Magnetron sputter vacuum deposition is the off-line process. Magnetron sputtering techniques such as radio frequency (RF), direct current (DC), and mid-frequency magnetron sputtering are widely used because of the advantage in obtaining good adhesion, good orientation and uniform films [14–16]. To obtain Al doped zinc oxide (AZO) thin films with the desired properties, deposition parameters such as sputtering power, deposition pressure, gas flux, substrate temperature, and the distance between target and substrate should be well determined and controlled. Although the influence of the pressure and sputtering power on the structural properties and postetching surface topography was studied [17], the performance and reliability of this technique require further investigation in order to meet the needs of industrial production. In this paper, high conductive and transparent ZnO:Al films were deposited by mid-frequency magnetron sputtering. The influence of the substrate temperature, working pressure, and sputtering power on the growth, electrical and optical properties was studied. The optimized films were applied as back reflectors in a-SiGe:H solar cells. The implementation of the ZnO:Al back reflector using the optimized deposition conditions resulted in an increase of 19% in the solar cell efficiency compared to a solar cell without the back reflector.

2 Experiment

AZO films were prepared on glass substrates by magnetron

sputtering technology in an in-line high vacuum deposition chamber. A ceramic target composed of ZnO:Al₂O₃ (98:2 wt%) was mounted on magnetron cathode in dynamic mode as the target can move forth and back in front of the substrate. The distance between substrate and target surface was approximately 60 mm. For all ZnO:Al films, the system was operated in mid-frequency mode with an excitation frequency of 20 KHz. The base pressure of the process chamber is less than 5×10^{-4} Pa. High purity argon was used as sputtering gas at a flow rate of 40 sccm. The sputtering power was varied from 80 to 180 W, and the argon gas pressure was controlled from 3 to 7 mTorr (mT) by throttle valves. The substrate temperature was varied from 150°C to 280°C. P-I-N a-SiGe thin film solar cells, which has a structure of glass/ZnO/p-type a-SiC:H/a-SiGe:H(i-layer)/n-type nano-crystalline silicon/ZnO/metal electrode, were fabricated using plasma enhanced chemical vapor deposition (PECVD) technology.

To study the optical properties, a 7-SCSpec solar spectroscopy system was used to measure the transmittance. The optical band gap (E_g) was determined by applying the Tauc model [18], in which E_g were deduced from the optical absorption spectra using the relation $(\alpha h\nu)^2 = (h\nu - E_g)$ by plotting $(\alpha h\nu)^2$ versus $h\nu$ and extrapolating the linear portion of the plot to $(\alpha h\nu)^2 = 0$, where α is the absorption coefficient, $h\nu$ is the photon energy. Electrical properties of the ZnO:Al films were characterized by Hall-effect measurement using van der Pauw geometry (Keithley 926 Hall set-up). The film resistivity was measured using a four point probe measurement system. The thicknesses were measured with a surface profiler (Dektak 3030 supplied by Veeco Instruments Inc.).

The active area of the cells was defined by the thermally

evaporated Al back contact and was about 0.253 mm². Current-voltage (I - V) characteristics were obtained using a solar simulator providing the AM 1.5 spectra. All measurements were performed at room temperature.

3 Results and discussion

3.1 Electrical properties

3.1.1 Influence of working pressure on electrical properties

The change of resistivity as a function of working pressure is shown in Fig. 1. From Fig. 1, it is observed that the resistivity is relatively high ($2.77 \times 10^{-4} \Omega \cdot \text{cm}$) at a low pressure (3 mTorr). As the working pressure increases to 4 mTorr, the resistivity decreases to $2.45 \times 10^{-4} \Omega \cdot \text{cm}$. However, as the working pressure increases further, the resistivity increases to $2.92 \times 10^{-4} \Omega \cdot \text{cm}$ at a working pressure of 7 mTorr. It is known that the resistivity is determined by the carrier concentration (Nh) and Hall mobility (μ_r). The influence of working pressure on the electrical properties is further investigated by the study of the carrier concentration and Hall mobility of the films. Figure 1 shows the carrier concentration and Hall mobility for the samples deposited at various working pressure. From the figure, it is presented that the film deposited at the pressure of 4 mTorr has the largest carrier concentration and Hall mobility. At working pressure of 3 mTorr, the carrier concentration is $1.27 \times 10^{20} \text{ cm}^{-3}$ and the Hall mobility is $62.4 \text{ cm}^2 \cdot \text{V}^{-1} \cdot \text{s}^{-1}$. With working pressure increasing to 4 mTorr, the carrier concentration increases to $3.2 \times 10^{20} \text{ cm}^{-3}$ and the Hall mobility increases to $69.3 \text{ cm}^2 \cdot \text{V}^{-1} \cdot \text{s}^{-1}$. However, as the working pressure increases

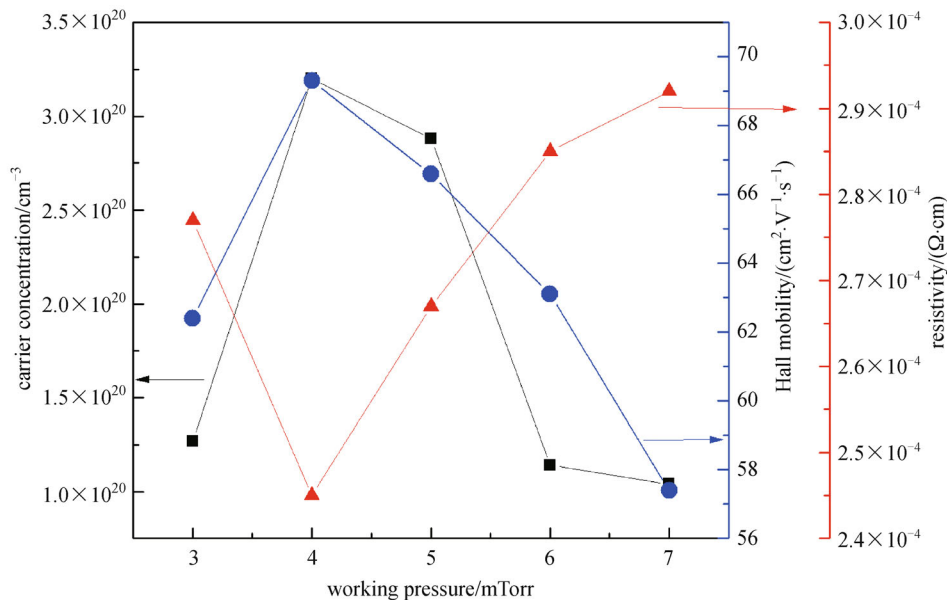


Fig. 1 Influence of working pressure on resistivity, carrier concentration and Hall mobility of AZO thin films

further, the carrier concentration and Hall mobility decrease to $1.04 \times 10^{20} \text{ cm}^{-3}$ and $57.4 \text{ cm}^2 \cdot \text{V}^{-1} \cdot \text{s}^{-1}$ at 7 mTorr.

In magnetron sputtering, the working pressure has the great influence on the density and energy of the sputtering particles [19]. With pressure increasing, the mobility of the growth radicals on the surface increases because of the increase of the energy of the sputtering particles. The growth radicals thus have the enough time to find suitable sites, resulting in the reducing of defect and the increasing of the grain size in the film. So, the carrier concentration in the film increases and the resistivity of the film decreases [19]. However, as the increase of working pressure exceeds a certain value, the sputtering particles colliding with argon atoms or ions becomes more frequent, which increases the scattering degree of the sputtering particles. The crystallinity of the films is thus deteriorated, leading to the reduction of the carrier concentration and Hall mobility.

3.1.2 Influence of substrate temperature on electrical properties

Figure 2 shows the resistivity, carrier concentration and Hall mobility of the films as a function of substrate temperature. As shown in the figure, the Hall mobility, carrier concentration is low and the resistivity is high at low substrate temperature of 150°C . At temperature of 150°C , the carrier concentration, Hall mobility and resistivity are $1.88 \times 10^{20} \text{ cm}^{-3}$, $22.6 \text{ cm}^2 \cdot \text{V}^{-1} \cdot \text{s}^{-1}$ and $1.51 \times 10^{-3} \Omega \cdot \text{cm}$ respectively. As substrate temperature increases to 225°C , a low resistivity of $2.45 \times 10^{-4} \Omega \cdot \text{cm}$ was obtained. However, as substrate temperature increases further, the resistivity increases. At substrate temperature

of 280°C , the resistivity is $6.08 \times 10^{-4} \Omega \cdot \text{cm}$ with carrier concentration of $2.3 \times 10^{20} \text{ cm}^{-3}$ and Hall mobility of $50.9 \text{ cm}^2 \cdot \text{V}^{-1} \cdot \text{s}^{-1}$. At a low substrate temperature, the mobility of the growth radicals is too low to move to the lowest energy location. The film with poor crystallization quality and a large amount of defect is thus formed. The mobility of the carriers is thus low and the resistivity of the film is high. As substrate temperature increases, the grain size is increased and the quality of the film is improved, which is beneficial for the reduction of the defect scattering in the grain boundary. Meanwhile, higher substrate temperature is conducive to the desorption of adsorptive oxygen at grain boundary and the substitution doping of Al, which is helpful for the increase of the carrier concentration. The resistivity of the film is thus decreased. However, as the substrate temperature increases further, the oxygen vacancy in the films is reduced.

3.1.3 Influence of sputtering power on electrical properties

Figure 3 shows the resistivity, carrier concentration, and Hall mobility of the AZO thin films as a function of sputtering power. From the figure, it is observed that the resistivity of the film showed a tendency to decrease with power. The resistivity decreased from 3.15×10^{-4} to $2.45 \times 10^{-4} \Omega \cdot \text{cm}$ when the sputtering power increases from 80 to 160 W. In addition, the carrier concentration decreases with power increasing. At power of 80 W, the carrier concentration is about $6.7 \times 10^{20} \text{ cm}^{-3}$. As power increases to 180 W, the carrier concentration decreases to $3.6 \times 10^{20} \text{ cm}^{-3}$. The Hall mobility increases first and then tends to decrease when the power exceeds 160 W. At the power of 80 W, the Hall mobility is about $5.2 \text{ cm}^2 \cdot \text{V}^{-1} \cdot \text{s}^{-1}$. With power increasing to 160 W, the Hall mobility increases to

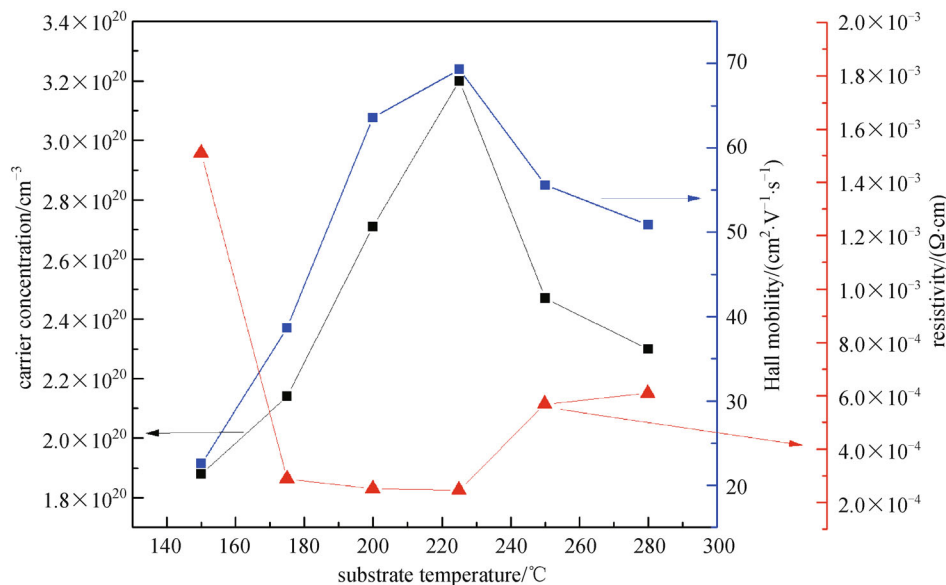


Fig. 2 Influence of substrate temperature on resistivity, mobility and Hall concentration of AZO thin films

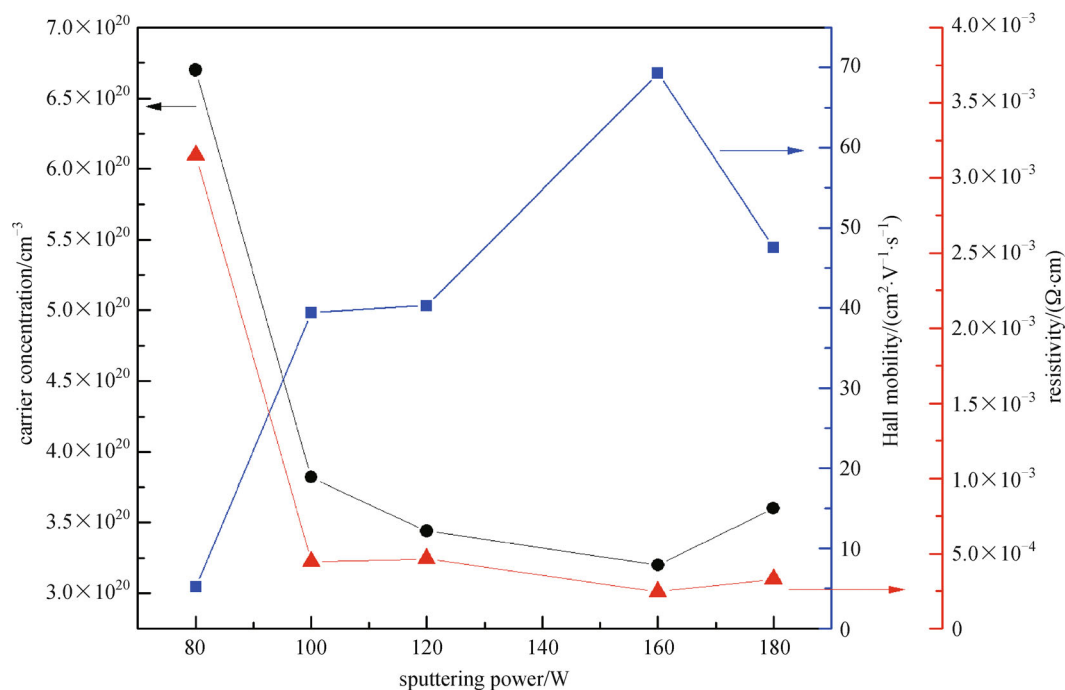


Fig. 3 Influence of sputtering power on resistivity, carrier concentration and Hall mobility of AZO thin films

69.3 cm²·V⁻¹·s⁻¹. With power further increasing to 180 W, the Hall mobility reduces to 47.6 cm²·V⁻¹·s⁻¹. The improved electrical properties are due to the desorption of negatively charged oxygen species from grain boundary surfaces [20]. In addition, the passivation of surface and defects at grain boundaries, which diminishes scattering and trapping of free carriers and enhances the doping effect of Al, also contributes to the conductivity of the film [21].

3.2 Optical properties

3.2.1 Influence of working pressure on optical properties

Figure 4 shows the optical transmission and optical band gap for the films deposited at various working pressures. As shown in the figure, the films deposited at lower pressure have the higher transmission and optical band

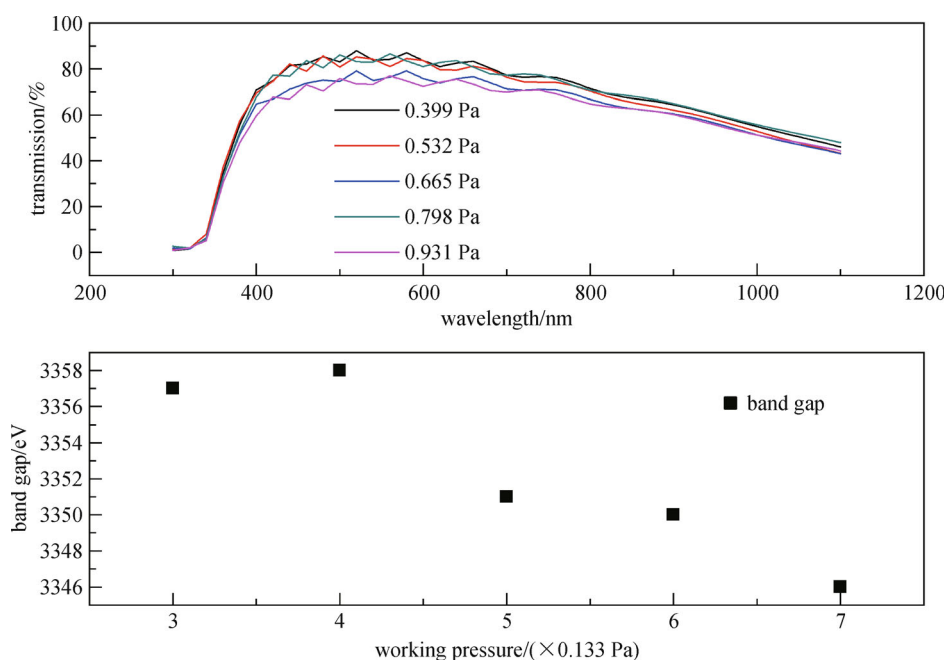


Fig. 4 Influence of working pressure on transmission and band gap of AZO thin films

gap. Also, it is observed that the transmission for all films decreases at long wavelength band. This phenomenon indicates that the films have the strong absorption at red band. It is reported that the doped AZO film has a phenomenon of band gap narrowing, in which the value of the shrinking of the band gap is proportional to $1/3$ power of the carrier concentration [22]. In Fig. 4, the curve corresponding to 0.5 Pa decreases rapidly in the long-wavelength, indicating that the carrier concentration is high and the absorption on the red end of the spectrum is strong for the film deposited at this pressure.

3.2.2 Influence of substrate temperature on optical properties

The influence of substrate temperature on the transmittance of the deposited film is shown in Fig. 5. As can be seen from Fig. 5, the difference of the transmittance in the visible range is very small. The largest optical band gap is obtained at 225°C. As the substrate temperature increases to exceed 225°C, the grain size on the surface and the film roughness increase, which leads to the increases of the diffuse reflection and the light scattering on the surface and the decrease of the transmittance in the long wavelength range.

3.2.3 Influence of sputtering power on optical properties

Figure 6 shows the optical transmittance spectra and optical band gap of the AZO thin films deposited at various powers. As shown in the figure, the transmittance decreases with the power. With sputtering power increas-

ing, the energy of the sputtering particles increases, resulting in the deterioration of the crystallization quality. The optical scattering in the grain boundary is thus increased. From the figure, it can be seen that the average optical transmittance of the films deposited at sputtering power < 160 W is more than 85% in the visible wavelength range. In the ultraviolet range, all the films exhibit a sharp absorption edge because of the onset of fundamental absorption of ZnO:Al. Figure 6 exhibits band gap of the AZO thin films shifted from 3.35 eV to above 3.75 eV with sputtering power. The broadened band gap may result from the increase of carrier concentration [23]. As sputtering power increases to exceed 160 W, the optical band gap decreases, leading to the enhancement of the light absorption and the decrease of the transmittance.

3.2.4 Properties of a-SiGe:H solar cells with and without ZnO:Al back reflector

The optimized ZnO:Al film was applied as the back contact in a-SiGe:H solar cells. The performance of the solar cell was compared to that of the solar cell deposited without the ZnO:Al back reflector. Figure 7 shows the structure of a-SiGe:H solar cells with (a) and without (b) ZnO:Al back reflector. I - V characteristics of solar cells both are presented in Fig. 8. Table 1 lists the values of parameters, such as open-circuit voltage (V_{OC}), short-circuit current density (J_{SC}), fill factor (FF), and efficiency (η). As demonstrated in Fig. 8, the solar cell with ZnO:Al back reflector shows an improvement in the photo-current and at the same time maintains a high FF and V_{OC} . The solar cells with and without ZnO:Al back reflector showed

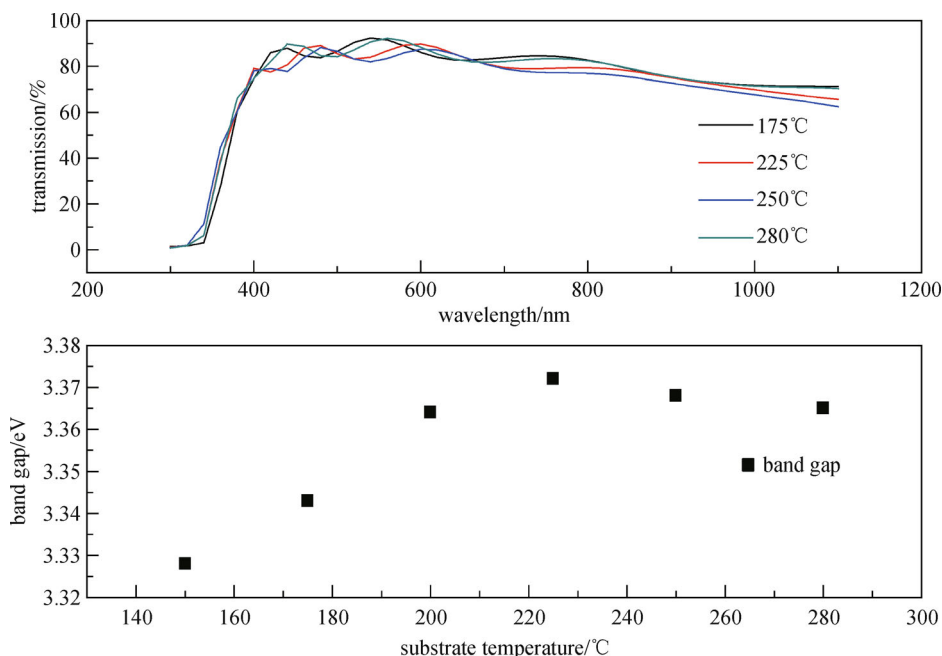


Fig. 5 Influence of substrate temperature on transmission and band gap of AZO thin films

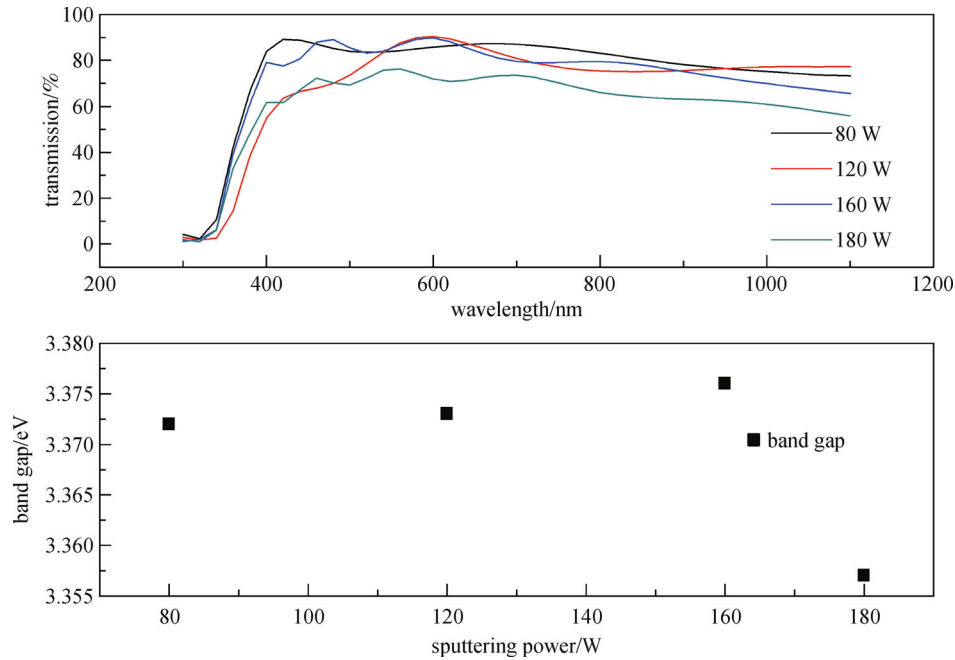


Fig. 6 Influence of sputtering power on transmission and band gap of AZO thin films

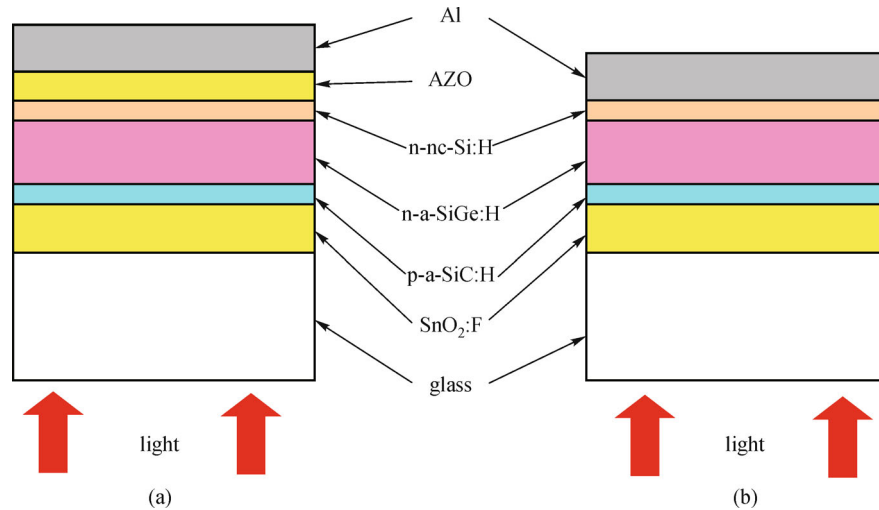


Fig. 7 Structure of a-SiGe:H solar cells with (a) and without (b) ZnO:Al back reflector

an efficiency of 8.51% and 7.15% respectively. Compared to the solar cell without back reflector, an enhancement of 19% in the efficiency is observed for the cell with ZnO:Al back reflector. For a-SiGe:H solar cells with AZO back reflector, the introducing of AZO layer between silicon layers and metal increases the reflectivity of the back reflector. Thus, an enhancement of efficiency is obtained.

4 Conclusions

AZO thin films were prepared by mid-frequency magne-

tron sputtering technique. The properties of the films were studied. Results suggest that the deposition parameters such as substrate temperature, working pressure, and sputtering power have the great influence on the electrical and optical properties of the films. AZO films with a resistivity of $2.45 \times 10^{-4} \Omega \cdot \text{cm}$ and optical transmission greater than 85% in visible spectrum region were obtained at the substrate temperature of 225°C and a low sputtering power of 160 W. The optimized films were applied as back reflectors in a-SiGe:H solar cells. A relative increase of 19% in the solar cell efficiency was achieved in comparison to the cell without the ZnO:Al.

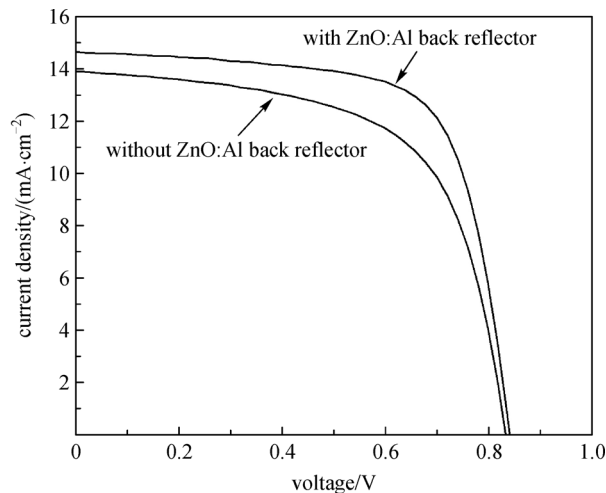


Fig. 8 I - V characteristics of a-SiGe:H solar cells with and without ZnO:Al back reflector

Table 1 Performances of p-i-n single junction a-SiGe:H solar cells prepared with and without AZO films back reflector

type	V_{oc}/V	$J_{sc}/(mA \cdot cm^{-2})$	FF	$\eta/\%$
without AZO back reflector	0.83	13.90	0.62	7.15
with AZO back reflector	0.84	14.65	0.70	8.51

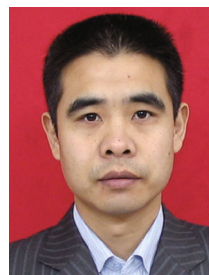
Acknowledgements This work was supported by Key Project of Natural Science Foundation of Hubei Province (No. 2009CBA025). The authors would like to thank Analytical and Testing Center of Huazhong University of Science and Technology.

References

- Nakagawara O, Kishimoto Y, Seto K, Koshido Y, Yoshino Y, Makino T. Moisture-resistant ZnO transparent conductive films with Ga heavy doping. *Applied Physics Letters*, 2006, 89(9): 091904-1–091904-3
- Bhosle V, Tiwari A, Narayan J. Metallic conductivity and metal-semiconductor transition in Ga-doped ZnO. *Applied Physics Letters*, 2006, 88(3): 032106-1–032106-3
- Vandendonker M, Gordijn A, Stiebig H, Finger F, Rech B, Stannowski B, Bartl R, Hamers E, Schlattmann R, Jongerden G. Flexible amorphous and microcrystalline silicon tandem solar modules in the temporary superstrate concept. *Solar Energy Materials and Solar Cells*, 2007, 91(7): 572–580
- Hao X T, Ma J, Zhang D H, Yang Y G, Ma H L, Cheng C F, Liu X D. Comparison of the properties for ZnO:Al films deposited on polyimide and glass substrates. *Materials Science and Engineering B*, 2002, 90(1–2): 50–54
- Vanheusden K, Warren W L, Seager C H, Tallant D R, Voigt J A, Gnade B E. Mechanisms behind green photoluminescence in ZnO phosphor powders. *Journal of Applied Physics*, 1996, 79(10): 7983–7990
- Chopra K L, Major S, Pandya D K. Transparent conductors—a status review. *Thin Solid Films*, 1983, 102(1): 1–46
- Granqvist C G. Window coatings for the future. *Thin Solid Films*, 1990, 193–194(Part 2): 730–741
- Zhang D H, Yang T L, Ma J, Wang Q P, Gao R W, Ma H L. Preparation of transparent conducting ZnO:Al films on polymer substrates by r.f. magnetron sputtering. *Applied Surface Science*, 2000, 158(1–2): 43–48
- Fortunato E, Nunes P, Marques A, Costa D, Águas H, Ferreira I, Costa M E V, Godinho M H, Almeida P L, Borges J P, Martins R. Transparent, conductive ZnO:Al thin film deposited on polymer substrates by RF magnetron sputtering. *Surface and Coatings Technology*, 2002, 151–152(1): 247–251
- Suzuki A, Matsushita T, Wada N, Sakamoto Y, Okuda M. Transparent conducting Al-doped ZnO thin films prepared by pulsed laser deposition. *Japanese Journal of Applied Physics*, 1996, 35(Part 2, No. 1A): L56–L59
- Minami T, Sato H, Sonohara H, Takata S, Miyata T, Fukuda I. Preparation of milky transparent conducting ZnO films with textured surface by atmospheric chemical vapour desposition using Zn ($C_5H_7O_2$)₂. *Thin Solid Films*, 1994, 253(1–2): 14–19
- Song J, Park I J, Yoon K H. Electrical and optical properties of ZnO thin films prepared by the pyrosol method. *Journal of the Korean Physical Society*, 1996, 29(2): 219–224
- Hu J H, Gordon R G. Textured aluminum-doped zinc oxide thin films from atmospheric pressure chemical-vapor deposition. *Journal of Applied Physics*, 1992, 71(2): 880–890
- Lai K C, Wang J H, Lu C H, Tsai F J, Yeh C H, Houng M P. Plasma-induced TCO texture of ZnO:Ga back contacts on silicon thin film solar cells. *Solar Energy Materials and Solar Cells*, 2011, 95(2): 298–305

415–418

15. Zhang W D, Bunte E, Ruske F, Kohl D, Besmehn A, Worbs J, Siekmann H, Kirchhoff J, Gordijn A, Hüpkas J. As-grown textured zinc oxide films by ion beam treatment and magnetron sputtering. *Thin Solid Films*, 2012, 520(12): 4208–4213
16. Chen X L, Wang F, Geng X H, Zhang D K, Wei C C, Zhang X D, Zhao Y. New natively textured surface Al-doped ZnO-TCOs for thin film solar cells via magnetron sputtering. *Materials Research Bulletin*, 2012, 47(8): 2008–2011
17. Kluth O, Schöpe G, Hüpkas J, Agashe C, Müller J, Rech B. Modified Thornton model for magnetron sputtered zinc oxide: film structure and etching behaviour. *Thin Solid Films*, 2003, 442(1–2): 80–85
18. Mandal S, Singha R K, Dhar A, Ray S K. Optical and structural characteristics of ZnO thin films grown by rf magnetron sputtering. *Materials Research Bulletin*, 2008, 43(2): 244–250
19. Ellmer K. Resistivity of polycrystalline zinc oxide films: current status and physical limit. *Journal of Physics D, Applied Physics*, 2001, 34(21): 3097–3108
20. Fang G J, Li D J, Yao B L. Fabrication and vacuum annealing of transparent conductive ZAO thin films prepared by DC magnetron sputtering. *Vacuum*, 2002, 68(4): 363–372
21. Oh B Y, Jeong M C, Myoung J M. Stabilization in electrical characteristics of hydrogen-annealed ZnO:Al films. *Applied Surface Science*, 2007, 253(17): 7157–7161
22. Wolff P A. Theory of the band structure of very degenerate semiconductors. *Physical Review*, 1962, 126(2): 405–412
23. Burstein E. Anomalous optical absorption limit in InSb. *Physical Review*, 1954, 93(3): 632–633



Qingsong Lei, Ph.D, was born in Hubei province, China, in February 1972. From September 1993 to July 1997, he studied in the Department of Materials Science and Technology, Lanzhou University, and received the bachelor of science degree. From September 2000 to July 2003, he studied in Lanzhou physics institute, China Academy of Space Technology, and received the master's degree in engineering. From September 2003 to October 2006, he studied in the Institute of Micro-Nano Science and Technology, Shanghai Jiao Tong University, and received the doctorate degree in engineering. From October 2006 to present, he is working in School of Optical and Electronic Information, Huazhong University of Science and Technology. The main research direction is silicon thin film solar cells.



Jiang Li, was born in Anhui province, China, in November 1990. From September 2008 to July 2012, he studied in the Department of Materials Physics, Harbin University of Science and Technology, and received the bachelor of science degree. From September 2012 to present, he is studying in School of Optical and Electronic Information, Huazhong University of Science and Technology. The main research direction is silicon thin film solar cells.